RSC Advances

ROYAL SOCIETY OF CHEMISTRY

www.rsc.org/advances

Ultra-low Dielectric Closed Porous Materials via Incorporating Surface-functionalized Hollow Silica Microspheres: Preparation, Interface Property and Low Dielectric Performance

Xiaonan Wei, Cuijiao Zhao, Jiajun Ma, Yawen Huang*, Ke Cao, Guanjun Chang, Junxiao Yang

State Key Laboratory Cultivation Base for Nonmetal Composite and Functional Materials, Southwest University of Science and Technology, Mianyang, 621010，China

Abstract: One effective route to reduce dielectric constant is to directly incorporate hollow silica ($HoSiO_2$) microspheres into polymeric matrix. However, the incompatibility between silica with hydrophobic polymers possibly results into interfacial defects and polarization, and thus high dielectric loss. In this study, the $HoSiO_2$ microspheres were coated by polystyrene using surface-initiated ATRP method in order to enhance interfacial property. TGA results indicated that the weight percentage of polystyrene in as-resulted microspheres ($HoSiO_2$@SI-PS) reached to around 33 wt.%. OM images showed that the thickness of polystyrene layer reached to around 2 μm. $HoSiO_2$@SI-PS microspheres with weight percentage of 25 % were incorporated into polyethylene (PE) to prepare composites. The dielectric measurement results indicated that the dielectric constant of the composites was reduced to 2.05, while maintaining low dielectric loss in the level of 10^{-4}. As compared, when $HoSiO_2$@C-PS microspheres, which were prepared by conventional vinyl-initiated free radical polymerization, were incorporated into polyethylene, the dielectric loss was greatly elevated to 0.007. SEM images and water absorption experiments further revealed that the low dielectric loss of PE/$HoSiO_2$@SI-PS was

*Corresponding author
Email addresses: huangyawen@swust.edu.cn (Y.W. Huang)

related to dense interfacial structure, strong interfacial interaction and low water absorption ability.

Keywords: hollow silica microspheres; surface-functionalization; interface property; ultra-low dielectric

INTRODUCTION

Low-k interconnect dielectrics have received significant attention from the microelectronics industry because their use in integrated circuits (ICs) can lower propagation delays, cross-talk noise, and power dissipation in interconnects. In the past few years, with the continuous scaling down of individual devices within integrated circuits, ultralow dielectric (k<2.0) materials have become the hot topic in this field. [1]

One way to reduce dielectric constant is incorporating nanopores into polymeric or inorganic matrix because the dielectric constant of pore is 1. [2-6] In the past few years, variety of porous low dielectric materials has been extensively studied. [7-21] These porous materials were generally prepared by incorporating decomposable groups or materials followed by thermal/UV or acid/alkaline treatment. The pores were facilely generated by removing the decomposable groups or moieties. Dang et al. [22] prepared nanoporous fluorinated polyimide by in situ polymerization process in the presence of SiO_2 nanoparticles followed by the removal of SiO_2 nanoparticles using HF acid etching. The dielectric constant was decreased to 2.45. However, dielectric loss was at the level of 10^{-2}. Loo et al. [23] prepared ultralow dielectric materials derived from poly(D,L-lactide-b-pentafluorostyrene) diblock copolymers. Ordered porous structure was attainable by removing PLA from the nanostructure induced from microphase separation. In particular, the current low-k materials used in volume manufacturing, which are porous organics-added silica, are also prepared based on above strategy. However, it should be noted that although low dielectric constant is achievable for most of current porous materials, high porosity is generally required and their pore structures are uncontrollable, opened or connected. As a result, these porous materials may exhibit poor water resistance, copper barrier performance and high dielectric

loss.

The incorporation of hollow particles[24-26] or cage-like molecules[27,28] into polymeric matrix provides an alternative route to porous materials. As compared with conventional porous materials, this method is facile and enables the formation of closed porous materials.[29] Hollow silica particles are ideal candidates to prepare this type of porous materials because they are industrialized and easy-attainable. However, as well-known, silica particles have poor compatibility with common polymer matrix, thus leading to poor interfacial property. This is definitely unfavorable to maintain the low dielectric loss of matrixes. Surface-functionalization method has been demonstrated available in enhancing mechanical, electrical/thermal conducting performance, etc. However, to the best of our knowledge, the effect of surface-functionalization on low-dielectric performance was not reported before.

Conventional vinyl-initiated polymerization is intrinsically a copolymerization between vinyl-functionalized SiO_2 and monomers.[30] As a result, the homopolymerization of monomers in solution is unavoidable. Thus, the grafting ratio of polymers is relatively low. In the past few years, surface-initiated free radical polymerization has demonstrated wide and important application in the surface-grafting of polymers on inorganic or organic particles.[31] This method allows to synthesis polymers in a controlled fashion, resulting in polymers with narrowly dispersed and controlled molecular weights. Herein, in this work, hollow SiO_2 microspheres (HoSiO$_2$) microspheres were surface-functionalized by PS using surface-initiated ATRP method. As-resulted HoSiO$_2$@PS microspheres were used to prepare PE composites. In addition, to show the characteristic feature of this porous material, other PE composites were prepared by incorporating MPS functionalized HoSiO$_2$ and HoSiO$_2$@PS microspheres prepared by conventional vinyl-initiated free radical polymerization (HoSiO$_2$@C-PS). The dispersion and interface property of hollow nanoparticles in PE, the porous structure of resulted composites, the corresponding low dielectric property, the water resistance and the mechanical property were compared and studied in detail.

EXPERIMENTAL

Chemicals

Hollow silica with an effective mean diameter of 20 μm was purchased from Guangzhou Chaotong Glass Product Trading Company Co. (Guangzhou, China). 3-Methacryloxypropyltrimethoxysilane (MPS) (>97%) and divinylbenzene (DVB, 80% divinylbenzene isomers) were purchased from Aladdin Chemistry Co. Ltd. Polyvinylpyrrolidone (PVP), triethylamine and dimethylaminopyridine (DMAP) were provided by Chengdu Kelong Chemical Reagent Factory. Polyethylene micropowder (PE, AR) was provided by Shanghai Youngling Electromechanical Technology Co., Ltd. (3-Glycidoxypropyl) trimethoxysilane (GPS) and N, N, N', N'', N''-pentamethyldiethylenetriamine (PMDETA) were purchased from Aladdin and used as received. 2-Bromoisobutyryl bromide (2-BriB, 98%) was used as received from Beijing G&K Technology Co., Ltd. Copper(II) bromide ($CuBr_2$, 99.8%) was provided by Chinese Medicine Group Chemical Reagent Co. Ltd. Styrene with analytical purity was supplied by Chengdu Kelong Chemical Industry Co. (Chengdu, China). In prior to use, styrene was washed with 5% aqueous sodium hydroxide and water, then dried over anhydrous magnesium sulfate and vacuum distilled. 2,2-Azobisisobutyronitrile (AIBN) was purchased from Chengdu Kelong Chemical Industry Co. and was recrystallized from methanol in prior to use. Copper(I) chlorine (CuCl, 99.99%) was purchased by Shanghai KeFeng Chemical Industry Co. (Chengdu, China). It was purified by ice acetic acid washing for 12 h followed by recrystallization from ethanol. Polyethylene micropowder (PE, AR) was provided by Shanghai Youngling Electromechanical Technology Co., Ltd.

Preparation of PS grafted $HoSiO_2$ microspheres by ATRP ($HoSiO_2$@SI-PS)

The surface-initiated ATRP (SI-ATRP) on $HoSiO_2$ was conducted according to reported method which involves three steps: the preparation of hydroxyl-functionalized $HoSiO_2$, bromo-functionalized $HoSiO_2$ and surface-initiated polymerization.[32] A typical experiment is as following: the silica suspension (1.6 g

HoSiO$_2$ suspended in 2.4 g NaOH solution (pH=11)) and (3-glycidoxypropyl)trimethoxysilane (GPS) (6.7 mL, 0.03 mol) were added to a two-necked round bottom flask with a mechanical stir bar and a reflux condenser. The mixture was stirred for 15 min at room temperature, then was refluxed at 100 ^{o}C and kept stirring for 24 h. The reaction mixture was then cooled down to room temperature and precipitated into ice methanol. The precipitate was purified by centrifugation in methanol and THF for four to five times at 8000 rpm. The solids were dried at 45 ^{o}C in vacuum oven.

The hydroxyl-functionalized HoSiO$_2$ (OH-HoSiO$_2$, 1.0 g) was dispersed in 17 mL THF (the concentration was kept below 65 mg mL^{-1}). The solution was charged into a two-necked round bottom flask with a constant pressure funnel and was oscillated for 15 min. Then, triethylamine (1.5 mL) and DMAP (0.001 mol, 0.11g) were added. The solution was oscillated for 30 min. 2-Bromoisobutyryl bromide (0.007 mol, 0.9 mL) was then added drop by drop at 0 ^{o}C. After the addition was completed, the solution was slowly heated up to room temperature and oscillated for 48 h. Then, the colloids were precipitated by adding drop wise to a methanol/H$_2$O mixture (3:1 vol). The bromo-functionalized silica particles (Br-HoSiO$_2$) were recovered by repeated washing and centrifugation with methanol. The recovered particles were dried overnight at 45 ^{o}C in vacuum oven.

Br-HoSiO$_2$ (1 g), Cu(I)Cl (0.043 g, 0.43 mmol) and Cu(II)Br$_2$ (0.008 g, 0.0347 mmol), styrene (23 mL, 0.2 mol) and PMDETA (100 μL, 0.476 mmol) were sequentially added to another flask under nitrogen atmosphere. The flask was then placed in an oil bath at 90 ^{o}C for 6 h. The mixture were diluted with THF and precipitated into an excess of ice methanol followed by filtration and washing. The final silica particles (HoSiO$_2$@PS) were dried at 45 ^{o}C in vacuum oven.

Preparation of PS grafted HoSiO$_2$ by conventional radical polymerization (HoSiO$_2$@C-PS)

The silica hollow microspheres (3 g) were dried in the oven and dispersed in ethanol (50 mL). The PH of this solution was tuned to 3~4 by adding acetic acid

glacial. Subsequently, MPS (0.45 g, 8.9 mmol) was added. The solution was stirred for 2 h at room temperature and was oscillated continuously for 20 h at 30 $^{\circ}$C. The mixture was filtered and the filtrate was washed with ethanol for three to four times. The MPS-modified silica particles were dried in a vacuum oven at 45 $^{\circ}$C.

0.50 g of MPS-HoSiO$_2$ microspheres were suspended in 35 mL of ethanol. Then, St (0.9 g, 0.0086 mol), PVP (0.06 g, 0.002 mmol) and AIBN (0.02 g, 0.12 mmol) were sequentially added. The reaction was conducted at 65 $^{\circ}$C for 4 h. The resultant microspheres were purified by repeated centrifugation in toluene and ethanol and dried in a vacuum oven at 45 $^{\circ}$C.

Preparation of PE composites

HoSiO$_2$@SI-PS microspheres were mixed with PE powders (the weight ratio of PE/ HoSiO$_2$@SI-PS is 3:1) at ambient temperature. Subsequently, the mixture was charged into a stainless mould with diameter of 2.5 cm. The samples were hot pressed at 150 °C for 1.5 h under a pressure of 60 N, then the film was cooled down to the room temperature. Finally, composited pallets with dimensions of 6.25 cm^2 areas and about 1.5 mm thickness were obtained. The PE, PE/HoSiO$_2$, PE/MPS-HoSiO$_2$ and PE/HoSiO$_2$@C-PS pallets were prepared using the same method (Scheme 1).
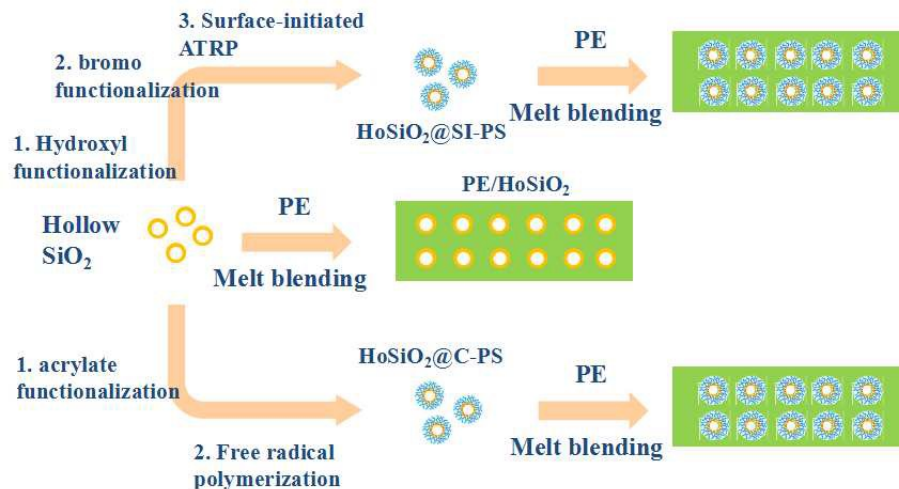
Scheme 1. Preparation routes to PE composites

Measurements

Fourier transform infrared (FTIR) measurements were conducted on a Nicolet FTIR 5700 spectrophotometer. Scanning electron microscopy analysis (SEM) images were obtained by means of Germany Zeiss Ultra 55 scanning electron microscope, the microstructure was observed under 15kV accelerating voltage. Optical microscopy analysis (OM) images was obtained by means of Japan Olympus BX051 Optical microscope. Thermalgravimetric analysis (TGA) was performed on a TGA Pyris 1, PE in flowing argon at a heating rate of 10 ^{o}C/min. The water adsorption was determined by follow method. The composite films were cut into square bricks with dimensions of 15 mm and immersed in water. The film was taken out at given time point, then dried and weighed. The water adsorption percentage was calculated by following equation:

$$W = (B - G)/G \times 100\%$$

Where W denotes the the water resistance, B and G denote respectively the weight of the film immersed and dried.

Mechanical properties were measured by Dynamic Mechanical Analysis (DMA) on Q800 (TA Instruments) working in the tensile mode. The sample dimensions were 1.5(thickness)×7(width)×10(effective length) mm^3 and tests were performed under isochronal conditions at 1 Hz and the temperature was varied between -145 ^{o}C and 110 ^{o}C at a heating rate of 7 ^{o}C min^{-1}.The dielectric permittivity and dielectric loss of the sample pallets were measured by Agilent 4294A Impedance Analyzer at various frequencies and ambient temperatures. In prior to measurement, the pallets were cut into cubic sheets and Cu electrodes were magnetron sputtered on both sides. The dielectric permittivity was calculated by following equation:

$$\varepsilon_r = (C \times d)/(\varepsilon_0 \times S)$$

where C, d and S denote respectively the capacitance, thickness and surface area of composite film. ε_0 denotes permittivity of free space and equals to 8.854×10^{-12} F/m.

RESULTS AND DISCUSSIONS

Preparation of PS-grafted HoSiO$_2$ microspheres

PS-grafted HoSiO$_2$ microspheres were prepared by surface-initiated atom transfer radical polymerization of styrene on HoSiO$_2$. This method allowed to synthesis polymers in a controlled fashion, resulting in polymers with narrowly dispersed and controlled molecular weights. Hollow silica microspheres with the diameter of 20 µm were used. FTIR spectrum of the particles prepared from ATRP showed characteristic adsorption bands of phenyl and alkyl structures in the range of 1400-1600 and 2900-3020 cm^{-1} respectively (Figure 1c). This result indicated that PS chains were successfully grafted onto the surface of hollow silica microspheres. SEM image showed a rough surface of microspheres (Figure 2d). This phenomenon also supported the surface coating of polystyrene. OM images showed that the thickness of spherical shell of HoSiO$_2$ microspheres is about 0.5 µm (Figure 3a). For HoSiO2@SI-PS microspheres, it is increased to around 2.5 µm (Figure 3b). Thus, the estimated thickness of the coated polymer was about 2 µm. TGA curve of HoSiO$_2$@SI-PS particles showed the characteristic decomposition of PS with T$_{5\%}$ around 380 ^{o}C (Figure 4). The residual weight was around 67.0 wt%, which revealed that the weight percentage of HoSiO$_2$ was around 67.0 wt%, thus the weight percentage of grafted PS was around 33.0 wt%.
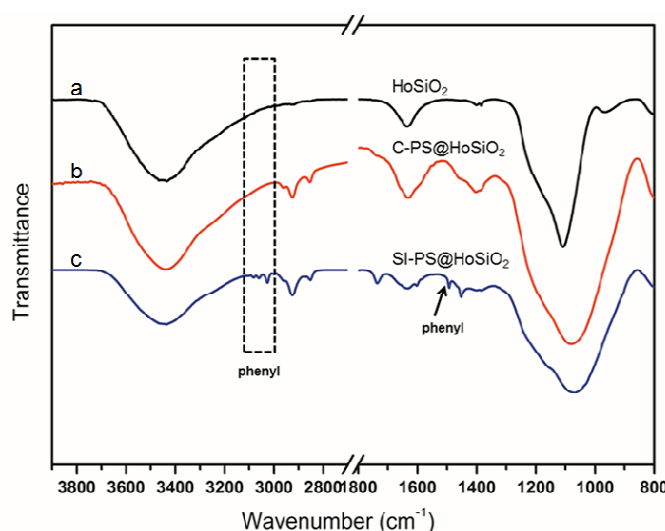
Figure 1. FT-IR spectra of HoSiO$_2$, HoSiO$_2$@C-PS and HoSiO$_2$@SI-PS.
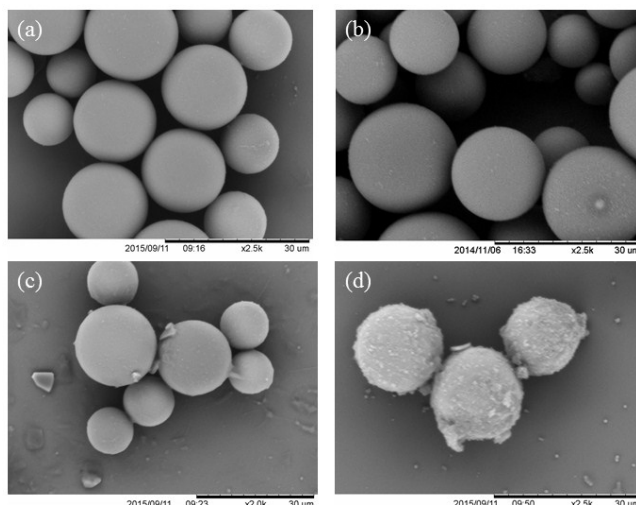
Figure 2. SEM images of HoSiO$_2$(a), MPS-HoSiO$_2$(b), HoSiO$_2$@C-PS(c) and HoSiO$_2$@SI-PS(d).
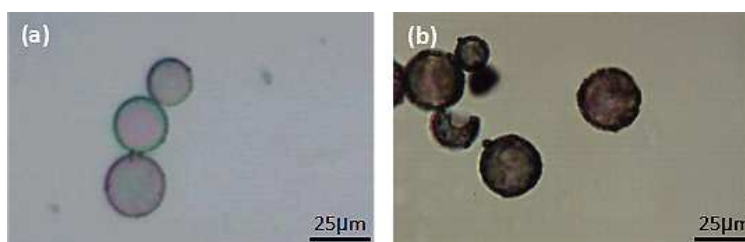
Figure 3. OM images of HoSiO$_2$ (a) and HoSiO$_2$@SI-PS (b) microspheres

As a comparison, a conventional method, which employs free radical polymerization of vinyl-functionalized HoSiO$_2$, was also used to prepare HoSiO$_2$@PS (HoSiO$_2$@C-PS). FTIR spectrum of HoSiO$_2$@C-PS showed an absence of adsorption band of phenyl groups in the range of 3000-3020 cm^{-1} and around 1500 cm^{-1}. SEM images of HoSiO$_2$@C-PS showed smooth surface like unmodified HoSiO$_2$. These results implied that few amount of PS was grafted onto the surface of HoSiO$_2$. This was further demonstrated by TGA curves of HoSiO$_2$@C-PS, which showed greatly high residual weight ratio around 99 %. One possible explanation for the low grafting ratio is possibly that large size of silica microspheres lowers the activity of vinyl groups.
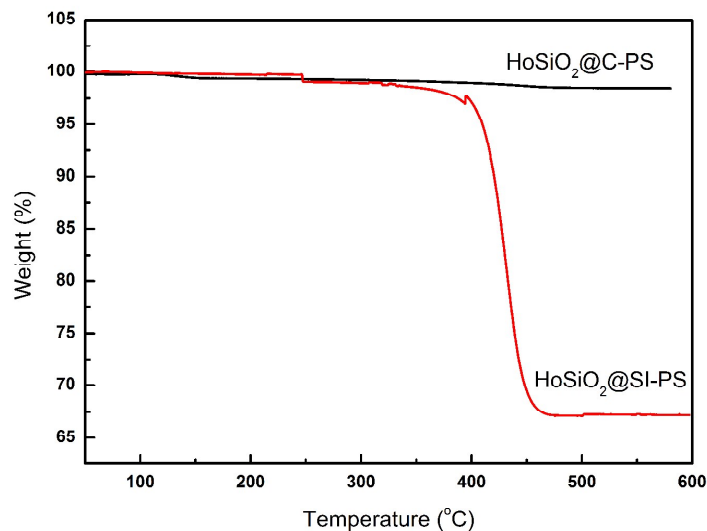
Figure 4. TGA curves of HoSiO$_2$@C-PS and HoSiO$_2$@SI-PS.

Preparation and interfacial property of PE/HoSiO$_2$@SI-PS composites

PE/HoSiO$_2$@SI-PS composite with HoSiO$_2$@SI-PS weight ratio of 3:1 was prepared by mechanical blending, followed by hot pressing. To make a comparison, PE/HoSiO$_2$, PE/MPS-HoSiO$_2$ and PE/HoSiO$_2$@C-PS composites with identical matrix/filler ratio were also prepared (Scheme 1). The morphology of the composites was characterized by SEM images of cross section surface. From the SEM image of PE/HoSiO$_2$@SI-PS, one can see that the HoSiO$_2$@SI-PS microspheres were uniformly dispersed in PE. No serious destruction of microspheres was observed. In other words, HoSiO$_2$ microspheres had adequate mechanical stability to maintain their hollow structure well after hot pressing. As a consequence, the pores were completely closed and isolated. Of particular important, the cross section morphology of PE/HoSiO$_2$@SI-PS composite showed apparent irregular plastics deformation morphology and highly rough fracture surfaces. The microspheres were well covered by PE matrix so that they were hardly peeled off during fracture of the composites. These phenomena suggested that PE chain possibly penetrated into PS shells during hot pressing, thus leading to a strong interfacial interaction.

From the SEM images of the PE/HoSiO$_2$, PE/MPS-HoSiO$_2$ and PE/HoSiO$_2$@C-PS composites, it can be seen that a considerable amount of microspheres were peeled off.

In addition, no plastics deformation and rough fracture surfaces was observed. These results pointed to a weak interfacial interaction. Besides, some microspheres were broken into small pieces, however, no irregular holes were observed. This phenomenon indicated that the breaking of the microspheres should take place during fracture of composites rather than hot pressing process. Apparently, the microspheres without PS coating exhibited poor mechanical stability.
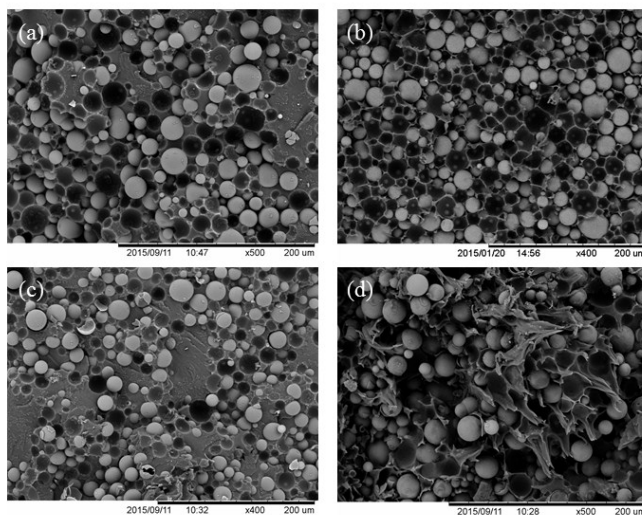
Figure 5. SEM images of cross section of PE composites. a) PE/HoSiO$_2$; b) PE/MPS-HoSiO$_2$; c) PE/HoSiO$_2$@C-PS; d) PE/HoSiO$_2$@SI-PS.

Water resistance and mechanical property of PE/HoSiO$_2$@SI-PS composites

The water adsorption curves with time are shown in Figure 6. It can be found that the PE/HoSiO$_2$@SI-PE composite exhibits greatly lower water adsorption as compared with PE/HoSiO$_2$. Possible explanation for this is that when HoSiO$_2$ microspheres are grafted with PS, their surface hydrophibility is greatly reduced. The low water adsorption is also possibly related to the dense interface, which inhibit the diffusion of water. In addition, the water adsorption of PE/HoSiO$_2$@SI-PE composite shows an increase till 12 h and almost kept at constant value (0.2%) after that point. This value is slightly higher than that of PE and is comparable with current industrialized low dielectric materials, demonstrating good water resistance of PE/HoSiO$_2$@SI-PE composite.
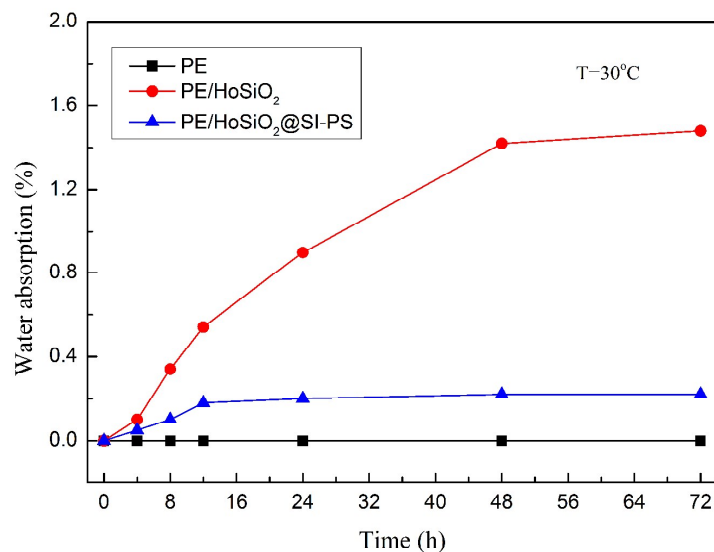
Figure 6. Water absorption of PE, PE/HoSiO$_2$ and PE/HoSiO$_2$@SI-PS composites with temperature at 30 ^{o}C. The contents of nanoparticles in composites were 25 wt.%.

Figure 7 showed the storage modulus of the pure PE, PE/HoSiO$_2$ and PE/HoSiO$_2$@SI-PS composites. In theory, when incorporating pores in matrix, the modulus is generated decreased. To our surprise, the storage modulus of PE/HoSiO$_2$ composite and PE/HoSiO$_2$@SI-PS composites are greatly higher than that of pristine PE, indicating higher stiffness. This high stiffness could be ascribed to the high stiffness of silica structure itself and also a reinforcing effect of HoSiO$_2$ microspheres.
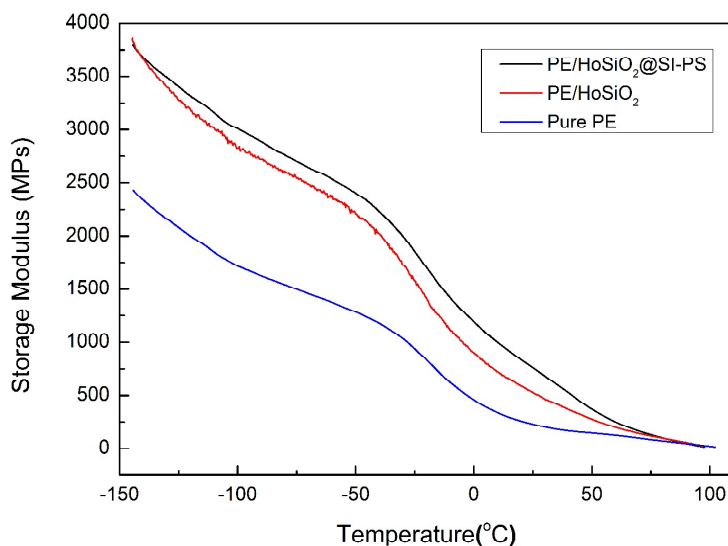
Figure 7. DMA curves of pure PE, PE/HoSiO$_2$ and PE/HoSiO$_2$@SI-PS composites.

Dielectric property of PE/HoSiO$_2$@SI-PS composites

In most of current studies, the highlight point is generally low dielectric constant of materials, while the dielectric loss is ignored. In fact, for future low dielectric used in interlayered/interlined packaging and high frequency related application, both of them are identically significant. Definitely, incorporating hollow SiO$_2$ microspheres into polymer matrix will effectively reduce dielectric constant in theory. However, at the same time, it will generate heterogeneous structure or introduce impurities, as a result, leading to elevated dielectric loss. Thus, the control of interfacial structure is of importance to optimize dielectric constant and loss. To show the impact of the control of interfacial structure on low dielectric property, the dielectric property of PE/HoSiO$_2$, PE/MPS-HoSiO$_2$ and PE/HoSiO$_2$@C-PS, where the HoSiO$_2$ have different coating structure, was compared and investigated in this work.

Table 1 summarizes the dielectric constant and loss of the PE/HoSiO$_2$, PE/MPS-HoSiO$_2$, PE/HoSiO$_2$@C-PS and PE/HoSiO$_2$@SI-PS composites at 10 MHz with (functionalized) HoSiO$_2$ weight ratio of 1:3. One can find that when HoSiO$_2$ and modified HoSiO$_2$ microspheres were incorporated into PE, the dielectric constants were commonly reduced. PE/HoSiO$_2$@SI-PS composites had relatively high dielectric constants as compared with PE/HoSiO$_2$. As indicated above, the HoSiO$_2$ in HoSiO$_2$@SI-PS is around 67 wt.%. As a result, the real weight percentage of HoSiO$_2$ in PE/HoSiO$_2$@SI-PS was relatively low than that in PE/HoSiO$_2$. This means that the porosity of PE/HoSiO$_2$@SI-PS was definitely lower than that of PE/HoSiO$_2$, thus leading to relatively high dielectric constant for PE/HoSiO$_2$@SI-PS composite. Besides, although the weight percentages of HoSiO$_2$ in PE/MPS-HoSiO$_2$ and PE/HoSiO$_2$@C-PS composites were close to that in PE/HoSiO$_2$ (TGA curve of HoSiO$_2$@C-PS indicated a 99 % residual ratio), the dielectric constants of PE/MPS-HoSiO$_2$ and PE/HoSiO$_2$@C-PS composites were apparently higher than that of PE/HoSiO$_2$. One possible explanation for this was that some impurities absorbed on the surface of HoSiO$_2$ owing to the presence of acrylate groups and uncovered hydroxyl groups (HoSiO$_2$ microspheres were treated by acid to form more hydroxyl

groups in prior to surface-functionalization).

Attractively, the dielectric loss of PE/HoSiO$_2$@SI-PS composite, which was at the level of 10^{-4}, was greatly close to that of PE. In contrast, the dielectric loss of PE/HoSiO$_2$@C-PS and PE/HoSiO$_2$ composites reached to the level of 10^{-3}. This result indicated that the dielectric loss is linked with the PS shell structure. When HoSiO$_2$ microspheres were grafted with adequate amount of PS chains, the interface dipolarization can be inhibited to a large degree. In addition, the surface was prevented from the absorption of polar matters such as water. This is also beneficial for decreasing dielectric loss.

Table 1. Dielectric constant and loss of PE, PE/HoSiO$_2$, PE/MPS-HoSiO$_2$, PE/HoSiO$_2$@C-PS and PE/HoSiO$_2$@SI-PS composites.

Samples	filler/PE weight ratios	Dielectric constant[a]	Dielectric loss[a]
PE	0	2.40	0.0002
PE/HoSiO$_2$	1:3	1.81	0.0014
PE/MPS-HoSiO$_2$	1:3	2.14	0.0080
PE/HoSiO$_2$@C-PS	1:3	2.10	0.0075
PE/HoSiO$_2$@SI-PS	1:3	2.05	0.0008

[a] Dielectric constant and loss were recorded at 10 MHz.

CONCLUSIONS

HoSiO$_2$ microspheres were surface-functionalized by polystyrene employing surface-initiated ATRP method. When these PS-coated HoSiO$_2$ microspheres were incorporated into PE with weight ratio of 1:3, the dielectric constant was reduced from 2.40 to 2.05. More attractively, the dielectric loss can also be reached to the level of 10^{-4}. Comparing experiments indicated that when MPS functionalized HoSiO$_2$ or derived PS functionalized HoSiO$_2$ by conventional vinyl-initiated free radical polymerization were used, the dielectric loss of resulted PE composites were greatly

enlarged. SEM images and water adsorption experiments revealed that the low dielectric loss was linked with dense interfaces and good water resistance. These results pointed to the significance of surface modification on enhancing low dielectric property. DMA results further showed that PE/HoSiO$_2$@SI-PS composite had higher storage modulus as compared with PE. The enhanced low dielectric property, water resistance and mechanical property by employing surface grafting provides a new insight for structure design of low dielectric materials. Further study on revealing the relationship between grafting density/chain length and low dielectric property is on-going in our group, possibly providing more detailed information on how to design interfacial structure for improving low dielectric performance.

Acknowledgement

REFERENCES

[1] W. Volksen, R. D. Miller and G. Dubois, *Chem. Rev.*, 2010, **110**, 56-110.

[2] Y. Boontongkong and R. E. Cohen, *Macromolecules*, 2002, **35**, 3647.

[3] L. M. Bronstein, S. N. Sidorov, P. M. Valetsky, J. Hartmann, H. Col-fen and M. Antonietti, *Langmuir*, 1999, **15**, 6256.

[4] R. S. Kane, R. E. Cohen and R. Silbey, *Chem. Mater.*, 1999, **11**, 90.

[5] V. Sankaran, J. Yue, R. E. Cohen, R. R. Schrock and R. J. Silbey, *Chem. Mater.*, 1993, **5**, 1133.

[6] B. H. Sohn, J. M. Choi, S. I. Yoo, S. H. Yun, W. C. Zin, J. C. Jung, M. Kanehara, T. Hirata and T. Teranishi, *J. Am. Chem. Soc.*, 2003, **125**, 632.

[7] H. Zhang, Q. G. Du, J. Zhou, X. L. Zhang, H. T. Wang and W. Zhong, *Eur. Polym. J.*, 2008, **44**, 1095-1101.

[8] B. F. Zhang and Z. G. Wang, *Chem. Mater.*, 2010, **22**, 2780-2789.

[9] B. H. Yang, H. Y. Xu, Z. Z. Yang and X. Y. Liu, *J. Mater. Chem.*, 2009, **19**, 9038-9044.

[10] C. H. Ji and F. Meng, *Macromolecules*, 2007, **40**, 2079-2085.

[11] C. M. Lew, R. Cai and Y. S. Yan, *Acc. Chem. Res.*, 2010, **43**, 210-219.

[12] T. L. Bucholz, S. P. Li and Y. L. Loo, *J. Mater. Chem.*, 2008, **18**, 530-536.

[13] S. Oh, J. K. Lee, P. Theato and K. K. Char, *Chem. Mater.*, 2008, **20**, 6974-6984.

[14] G. D. Fu, E. T. Kang, Z. L. Yuan, K. G. Neoh, D. M. Lai and A. C. H. Huan, *Adv. Funct. Mater.*, 2005, **15**, 315-322.

[15] W. C. Wang, E. T. Kang, R. H. Vora, K. G. Neoh, C. K. Ong and L. F. Chen, *Adv. Mater.*, 2004, **16**, 54-57.

[16] T. M. Long and T. M. Swager, *J. Am. Chem. Soc.*, 2003, **125**, 14113-14119.

[17] B. H. Yang, H. Y. Xu, Z. Z. Yang and C. Zhang, *J. Mater. Chem.*, 2010, **20**, 2469.

[18] T. Fukumaru, T. Fujigaya and N. Nakashima, *Polym. Chem.*, 2012, **3**, 369-376.

[19] M. Seino, W. Wang, J. E. Lofgreen, D. P. Puzzo, T. Manabe and G. A. Ozin, *J. Am. Chem. Soc.*, 2011, **133**, 18082-5.

[20] G. D. Fu, Z. Shang, L. Hong, E. T. Kang and K. G. Neoh, *Adv. Mater.*, 2005, **17**, 2622-2626.

[21] F. Goethals, I. Ciofi, O. Madia, K. Vanstreels, M. R. Baklanov, C. Detavernier, P. Van Der Voort and I. Van Driessche, *J. Mater. Chem.*, 2012, **22**, 8281.

[22] J. W. Zha, H. J. Jia, H. Y. Wang and Z. M. Dang, *J. phys. chem. c*, 2012, **116**, 23676-23681.

[23] T. L. Bucholz, S. P. Li and Y. L. Loo, *J. Mater. Chem.*, 2008, **18**, 530-536.

[24] G. F. Zhao, T. Ishizaka, H. Kasai, M. Hasegawa, T. Furukawa, H. Nakanishi and H. Oikawa, *Chem. Mater.*, 2009, **21**, 419–424.

[25] S. P. Mukherjee, D. Suryanarayana and D. H. Strope, *J. Non-Cryst. Soilds*, 1992, **783**, 147–148.

[26] D. X. Zhuo, A. G. Gu, Y. Z. Wang, G. Z. Liang, J. T. Hu, L. Yuan and W. Yao,

Polym. Adv. Technol., 2012, **23**, 1121-1128.

[27] W. H. Zhang, J. D. Xu, X. S. Li, G. H. Song and J. X. Mu, *J. Polym. Sci. Polym. Chem*., 2014, **52**, 780-788.

[28] Y. W. Chen, L. Chen, H.R. Nie and E. T. Kang, *J. Appl. Polym. Sci*., 2006, **99**, 2226-2232.

[29] M. Ree, J. H. Yoon and K.Y. Heo, *J. Mater. Chem*., 2006, **16**, 685-697.

[30] G. D. Fua, G. L. Li, K. G. Neohb and E. T. Kang, *Prog. Polym. Sci*., 2011, **36**, 127-167.

[31] S. K. Kumar, N. Jouault, B. Benicewicz and T. Neely, *Macromolecules*., 2013, **46**, 3199-3214.

[32] G. L. Chakkalakal, M. Alexandre, C. Abetz, A. Boschetti-de-Fierro and V. Abetz, *Macromol. Chem. Phys*., 2012, **213**, 513-528.

Graphical Abstract